# Marine Heat Waves

## Identification

### 1. Indicator Description

This indicator examines several characteristics of marine heat waves in U.S. coastal waters from 1982 to 2023. As average sea surface temperatures (SST) across the globe rise, scientists expect marine heat waves to increase in intensity, frequency, and duration (Cooley et al., 2022). These events have been associated with a variety of impacts, including shifts in species ranges, local extinctions, and economic impacts from declines in fisheries and damage to aquaculture (Frölicher & Laufkötter, 2018; Hobday et al., 2016; Mills et al., 2023; Smith et al., 2021).

Components of this indicator include:

- Change in annual cumulative intensity of marine heat waves from 1982 to 2023 (Figure 1).
- Change in cumulative intensity of marine heat waves by season from 1982 to 2023 (Figure 2).
- A detailed look at the severity of marine heat waves for covered U.S. coastal regions from 1982 to 2023 (Figure 3).
- A detailed timeline of marine heat waves at five selected marine protected areas along the U.S. coastline from 1982 to 2023 (Figure 4).

### 2. Revision History

June 2024: Indicator published.

## Data Sources

### 3. Data Sources

Data for this indicator were obtained from the National Oceanic and Atmospheric Administration's (NOAA's) National Centers for Environmental Information (NCEI). NCEI maintains an "optimum interpolation" daily gridded dataset of SST. The dataset incorporates observations from satellites, ships, buoys, and Argo floats into a 1/4° resolution near-global grid. Data for all figures relied on daily Optimum Interpolation SST version 2.1 (OISST v2.1), which covers the years 1981 to present and was described by Banzon et al. (2016). Data for the figure were retrieved from NCEI's website and processed by EPA.

### 4. Data Availability

The daily SST data used in this analysis are available for download from NOAA's NCEI at: www.ncei.noaa.gov/products/optimum-interpolation-sst. The data employed in the current analysis were downloaded in March 2024 from NCEI (2024).

# Methodology

## 5. Data Collection

Prior to 1980, ships were the predominant source of observation for SST, which provided only enough data for coarse-scale analyses of ocean temperatures. Starting in 1981, satellite-based observations became available from an infrared instrument, the Advanced Very High Resolution Radiometer (AVHRR), which provides daily, global coverage of SST. OISST v2.1 relies primarily on AVHRR observations to construct a gridded, 1/4° resolution, global, daily SST dataset from 1981 to present. AVHRR data are collected from Pathfinder 5.0/5.1 and U.S. Navy satellites, which have data available from 1981 to 2006 and 2006 to present, respectively.

*In situ* observations from ships, Argo floats, and buoys are combined with the satellite data using optimum interpolation to fill gaps on the grid and create a spatially complete map of SST. Additional bias corrections are made to the infrared SST data using buoy and ship observations as reference. For ice-covered regions, where there tend to be minimal *in situ* data, proxy SSTs are generated from sea ice concentrations.

A detailed summary of OISST v2 methodology is provided by Banzon et al. (2016). Huang et al. (2021) describe methodological updates associated with OISST v2.1.

This indicator starts in 1982 because that was the first year with complete data available; 1981 was incomplete.

## 6. Indicator Derivation

This analysis defines marine heat waves as anomalously warm events in which SST exceeds the 90$^{th}$ percentile climatology based on a 30-year historical baseline period (1982–2011) for at least five consecutive days (Hobday et al., 2016). Thresholds are calculated and applied for each individual day and each pixel on the map—thus, for example, the temperature on August 15 at a particular location is compared with the historical distribution of August 15 temperatures at that location. EPA used OISST v2.1 daily gridded SST data to identify marine heat wave events using an R software package ("heatwaveR") from Schlegel and Smit (2018), available at: https://robwschlegel.github.io/heatwaveR. The heatwaveR package makes it possible to calculate the frequency, duration, and intensity (extent to which the threshold has been exceeded) of marine heat waves.

The heatwaveR package includes the following procedures, as described by Hobday et al. (2016):

- A moving average window of 31 days is used for smoothing climatology and thresholds. A window width of 11 days, with five days on either side of the day being analyzed, is also used for the pooling of values and the calculation of climatology and threshold percentile for each day.

- If there is a gap of two or fewer days between two marine heat wave events, the script combines these events into one marine heat wave.

Source data are available for all ocean pixels worldwide. Figures 1 and 2 show results within the U.S. exclusive economic zone (EEZ), which extends up to 200 nautical miles offshore from the coast.

Figures 3 and 4 reflect an additional calculation of heat wave severity, using heat wave severity categories defined by Hobday et al. (2018) and illustrated in Figure TD-1, which is adapted from that publication. Figure TD-1's "Climatology" line represents the mean SST for a hypothetical location over the course of a year (or part of a year), based on the 30-year long-term reference period. The "Climatology" line peaks in the summer in the Northern Hemisphere; however, water temperatures can lag the standard definitions of seasons by a few months. Figure TD-1 also shows a 90$^{th}$ percentile line, again based on the distribution of measurements recorded at the location in question on each individual day of the year during the 30-year reference period.

Figure TD-1 shows the four categories of heat wave severity that this indicator uses. All four are fundamentally based on the temperature difference between the historical mean and the historical 90$^{th}$ percentile. For example, if the 90$^{th}$ percentile was 2 degrees warmer than the mean, then a heat wave event with a maximum temperature difference of 5 degrees above the mean would fall into Category II (strong) because 5 is more than two times 2 degrees, but less than three times. In this same example, an event would require a maximum temperature difference that is greater than 8 degrees above the mean in order to fall into Category IV (extreme).

**Figure TD-1. Conceptual Illustration of Marine Heat Wave Severity Categories**

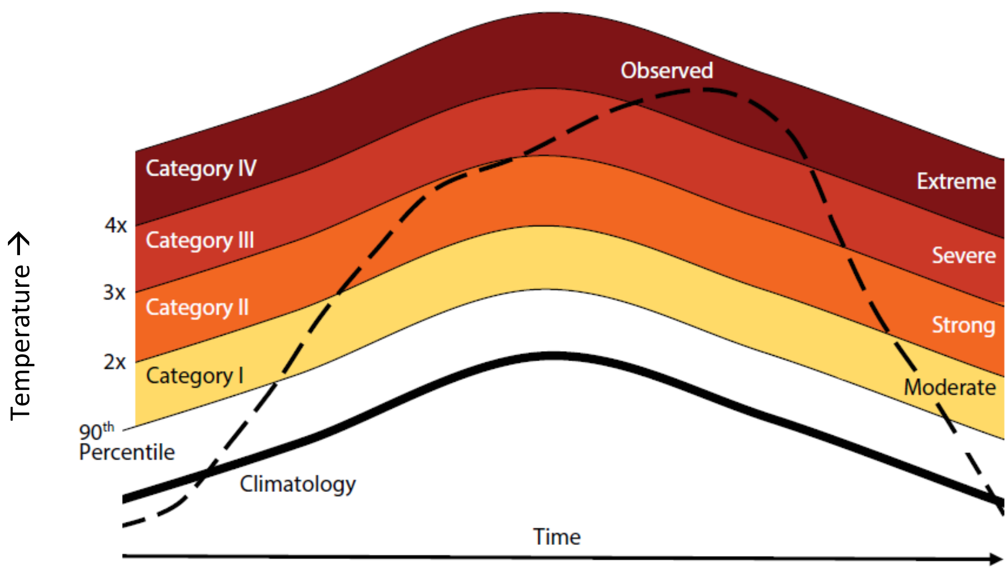


Source: Hobday et al. (2018)

Per the category definitions shown above, the absolute temperature threshold for what constitutes a moderate, strong, etc. heat wave varies by location and by season.

*Figure 1. Change in Annual Cumulative Intensity of Marine Heat Waves in the United States, 1982–2023*

For Figure 1, EPA focused on cumulative intensity as a way to consider both duration and intensity in a single metric. Cumulative intensity is determined by summing all daily intensities, which are the number of degrees above the historical 90$^{th}$ percentile for those days, for a marine heat wave. For example, an event lasting five days with intensities of 3, 2, 4, 5, and 1 °F would have a cumulative intensity of 15°F-days. To measure total change, EPA aggregated cumulative intensity by year for each grid cell of the EEZ before using a linear regression to calculate the long-term trend at each cell. The slope of each grid cell's trend (i.e., the rate of change per year) was multiplied by the number of years in the period to derive an estimate of total change.

*Figure 2. Change in Cumulative Intensity of Marine Heat Waves in the United States by Season, 1982–2023*

Figure 2 uses the same analytical approach as Figure 1 except that the trends are calculated by season. Figure 2 covers the same geographic area (EEZ) and overall timeframe as Figure 1, and the analysis has been replicated by three-month meteorological season (spring = March/April/May, and so on). Note that because meteorological winter (December/January/February) spans two calendar years, and data were not available for December 1981, the first winter shown is the one that started in December 1982, which is conventionally labeled “winter 1983.” If a single marine heat wave event spanned across multiple seasons or years, this analysis counted it one time and attributed its characteristics to the period in which the day with peak intensity occurred.

*Figure 3. Areas Affected by Marine Heat Waves by U.S. Coastal Region, 1982–2023*

Figure 3 provides a set of stacked graphs that shows the spatial extent of marine heat waves and their relative level of severity. Data are displayed by region, with regions defined as shown in the locator map attached to Figure 3. For each region, calculations were applied to all pixels within the EEZ that had OISST data.

Figure 3 shows the percentage of each coastal region’s area that experienced at least one marine heat wave in a given year. The stacked segments show severity levels categorized by color (see definitions in Figure TD-1) for the most severe heat wave experienced at a location in any given year, while the total height of the stack represents the total percentage area covered that experienced at least one marine heat wave of any severity. These graphs characterize the severity of each year’s most severe heat wave in recognition of the ecological importance of severity (i.e., a few severe or extreme heat waves could be more damaging than numerous moderate heat waves). For the purposes of Figure 3, this calculation is performed on the single day within each multi-day heat wave that has the maximum difference above the 90$^{th}$ percentile, meaning severity categorization is based on the peak conditions for any given heat wave.

All identification and classification of heat waves for Figure 3 was performed at the individual pixel level. Marine heat waves were identified if the temperature was higher than the historical 90$^{th}$ percentile threshold for at least five consecutive days, consistent with the definition used throughout this indicator. The resulting graphs in Figure 3 show what percentage of each region’s pixels experienced a heat wave in each year.

*Figure 4. Marine Heat Wave Intensity and Duration at Five Marine Protected Areas, 1982–2023*

Figure 4 examines marine heat wave patterns in five specific marine protected areas (MPAs): Kachemak Bay in Alaska, Olympic Coast in Washington, Florida Keys in Florida, Gerry E. Studds/Stellwagen Bank in Massachusetts, and Papahānaumokuākea in Hawaii. EPA elected to focus on these relatively small areas because larger region-wide averages could obscure and potentially undercount specific events (see Section 9, “Data Limitations”). The analysis uses MPAs because they are defined areas noted to have particular ecological value and sensitivity. EPA chose these five particular MPAs because they are located in five different coastal regions, thus offering a sampling of how marine heat waves are affecting a variety of coastal ecosystem types, from the coral reefs of South Florida to the cold and biologically productive Kachemak Bay in Alaska. Computationally, trends are based on conditions averaged across all the ocean pixels that are entirely or partially contained within the MPA boundary.

For more information about MPAs, see NOAA's website at: [https://marineprotectedareas.noaa.gov](https://marineprotectedareas.noaa.gov) and specifically NOAA's map viewer at: [https://marineprotectedareas.noaa.gov/dataanalysis/mpainventory/mpaviewer](https://marineprotectedareas.noaa.gov/dataanalysis/mpainventory/mpaviewer).

The graphs in Figure 4 show a discrete column for each individual heat wave event. Time is on the x-axis, so column width represents duration and the number of columns within a given timeframe represents frequency. Column height indicates intensity, and shading represents severity, using the same severity classes described in Figure TD-1 above.

*Indicator Development*

For reference, Figure TD-2 shows another approach for displaying regional information using the same marine heat wave definition used throughout this indicator. It quantifies the percentage area within a geographic region (in this case, the Northeast region as depicted in Figure 3) that experienced a marine heat wave in each month of each year. This analysis provides a sense of the area covered by marine heat waves for each month over the period of record. For this analysis, a marine heat wave is attributed to a month if it occurred any time during that month. EPA provides this additional diagnostic analysis as a basis for comparison to Figure 3 and in response to comments from the external peer review of this indicator on the relevance of inter-annual and seasonal differences in marine heat wave activity.

**Figure TD-2. Percent Area of the Northeast That Experienced a Marine Heat Wave, 1982–2023**

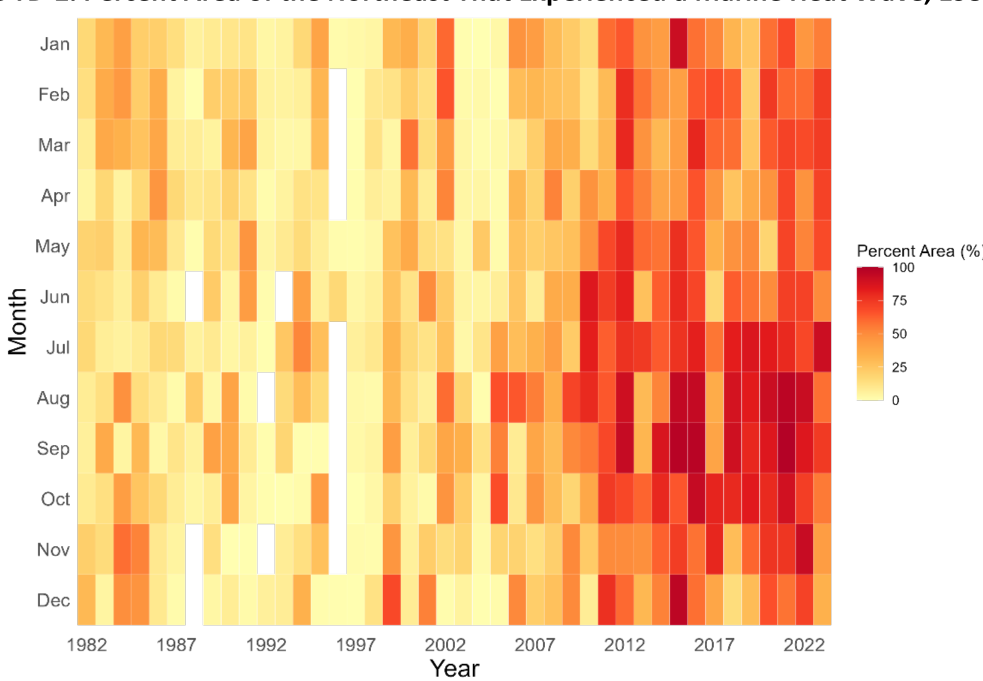


Data source: NOAA (2024)

## 7. Quality Assurance and Quality Control

Thorough documentation of quality assurance and quality control methods and results is available in the data citations under the "about" page for OISST v2.1 (www.ncei.noaa.gov/products/optimum-interpolation-sst).

# Analysis

## 8. Comparability Over Time and Space

Analytical methods have been applied consistently to all grid cells and all regions across all years of data. Each grid cell has a unique location-specific temperature threshold for defining a marine heat wave, but all such thresholds were calculated in the same manner with the same percentile ($90^{th}$) applied, as described in Section 6.

While analysis methods for the figure have not changed over the period of record, NOAA did update OISST from v2.0 to v2.1 from January 2016 onwards. This means SST data from 2016 onward were created using slightly different methods from the SST record for prior years. Some of these method updates include incorporating Argo float observations, reducing estimated ship SST bias, and switching the type of some ship and buoy observations used (Huang et al., 2021). These updates have helped to reduce overall bias and ensure a more accurate product from 2016 to the present.

## 9. Data Limitations

Factors that may affect the confidence, application, or conclusions drawn from this indicator are as follows:

1. OISST v2.1 (2016 to present) may have a residual SST cold bias of about -0.04°C over the global oceans and about -0.08°C in the Indian Ocean. This outcome may result from residual biases of satellite measurements that cannot be resolved by the bias correction algorithm in OISST or from nonhomogeneous *in situ* measurements from ships, buoys, and Argo floats.

2. OISST v2.0 (1982 to mid-2016) exhibited a slight cold bias in the Indian, South Pacific, and South Atlantic Oceans that is due to a lack of ingested drifting-buoy SSTs in the system. These biases were reduced in the OISST v2.1 update of data from 2016 to present.

3. Calculations using region-wide averages might not detect a more localized heat wave within the region, and they might understate the severity of a particular heat wave event if waters elsewhere in the region are not as anomalously warm at the same time. To address this limitation, EPA focused Figure 4 on five specific locations rather than calculate region-wide average conditions. The MPAs selected for Figure 4 are not necessarily representative of conditions along the entire coastline, but as case studies, they should effectively capture actual location-specific conditions.

## 10. Sources of Uncertainty

OISST has largely corrected for measurement error, but some uncertainty still exists. Contributing factors include AVHRR sensitivity to diurnal heating and to contamination by clouds and aerosols as well as instrument error from buoys and ships. Beggs (2020) noted that overall, OISST measurements do not align as well with Argo float data alone as other daily SST datasets do.

## 11. Sources of Variability

SST varies seasonally, but because Figure 1 is based on annual averages, it does not reveal the seasonal signal. EPA provides Figure 2 to show seasonal differences for context. Temperatures can also vary as a result of inter-annual climate patterns, such as the El Niño–Southern Oscillation.

## 12. Statistical/Trend Analysis

Figure 1 shows total change for each ocean pixel based on an ordinary least-squares linear regression of all years of data starting in 1982. The use of linear regression represents a first-order statistical assessment of significance. Further investigation could include testing the data for linearity and applying additional statistical testing accordingly.

Figure TD-3 shows the statistical significance of the 1982–2023 linear trend calculated for each pixel in Figure 1. The map reveals that almost the entire East Coast, Gulf Coast, and waters around Alaska and Hawaii have experienced long-term changes in annual cumulative heat wave intensity that are significant to at least a 95 percent level ($p < 0.05$)—and in many cases, significant to a much higher level. The changes on these parts of the map are predominantly increases (see Figure 1 of this indicator). Conversely, long-term linear trends for most of the West Coast are not significant.

**Figure TD-3. Statistical Significance of Trends Shown in Figure 1**

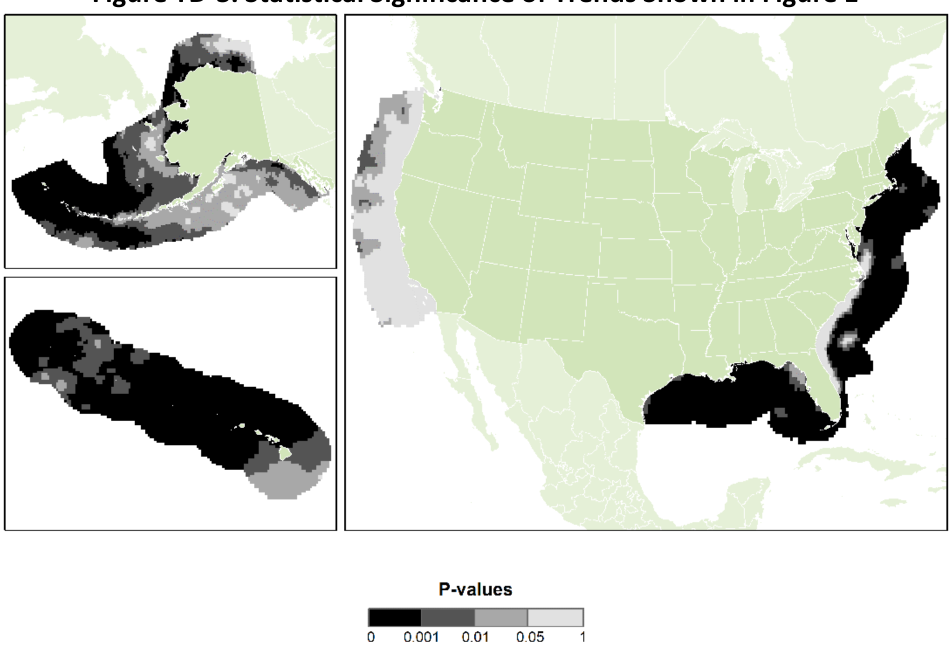


Data source: NOAA (2024)

## References


Banzon, V., Smith, T. M., Chin, T. M., Liu, C., & Hankins, W. (2016). A long-term record of blended satellite and in situ sea-surface temperature for climate monitoring, modeling and environmental studies. *Earth System Science Data*, *8*(1), 165–176. https://doi.org/10.5194/essd-8-165-2016

Beggs, H. (2020). Chapter 14: Temperature. In B. A. Harrison, J. A. Anstee, A. Dekker, S. Phinn, N. Mueller, & G. Byrne (Eds.), *Earth observation: Data, processing and applications: Vol. 3B: Applications—Surface waters* (pp. 292–330). Cooperative Research Centre for Spatial Information.

Cooley, S., Schoeman, D., Bopp, L., Boyd, P., Donner, S., Ghebrehiwet, D. Y., Ito, S.-I., Kiessling, W., Martinetto, P., Ojea, E., Racault, M.-F., Rost, B., & Skern-Mauritzen, M. (2022). Chapter 3: Oceans and coastal ecosystems and their services. In IPCC (Intergovernmental Panel on Climate Change), *Climate change 2022—Impacts, adaptation and vulnerability: Working Group II contribution to the Sixth Assessment Report of the Intergovernmental Panel on Climate Change*. Cambridge University Press. https://doi.org/10.1017/9781009325844.005

Frölicher, T. L., & Laufkötter, C. (2018). Emerging risks from marine heat waves. *Nature Communications*, *9*(1), 650. https://doi.org/10.1038/s41467-018-03163-6

Hobday, A. J., Alexander, L. V., Perkins, S. E., Smale, D. A., Straub, S. C., Oliver, E. C. J., Benthuysen, J. A., Burrows, M. T., Donat, M. G., Feng, M., Holbrook, N. J., Moore, P. J., Scannell, H. A., Sen Gupta, A., & Wernberg, T. (2016). A hierarchical approach to defining marine heatwaves. *Progress in Oceanography*, *141*, 227–238. https://doi.org/10.1016/j.pocean.2015.12.014

Hobday, A. J., Oliver, E. C. J., Sen Gupta, A., Benthuysen, J. A., Burrows, M. T., Donat, M. G., Holbrook, N. J., Moore, P. J., Thomsen, M. S., Wernberg, T., & Smale, D. A. (2018). Categorizing and naming marine heatwaves. *Oceanography*, *31*(2), 162–173. https://doi.org/10.5670/oceanog.2018.205

Huang, B., Liu, C., Banzon, V., Freeman, E., Graham, G., Hankins, B., Smith, T., & Zhang, H.-M. (2021). Improvements of the Daily Optimum Interpolation Sea Surface Temperature (DOISST) version 2.1. *Journal of Climate*, *34*(8), 2923–2939. https://doi.org/10.1175/JCLI-D-20-0166.1

Mills, K. E., Osborne, E. B., Bell, R. J., Colgan, C. S., Cooley, S. R., Goldstein, M. C., Griffis, R. B., Holsman, K., Jacox, M., & Micheli, F. (2023). Chapter 10: Ocean ecosystems and marine resources. In USGCRP (U.S. Global Change Research Program), *Fifth National Climate Assessment*. https://doi.org/10.7930/NCA5.2023.CH10

NOAA (National Oceanic and Atmospheric Administration). (2024). *Optimum interpolation SST*. Retrieved March 1, 2024, from www.ncei.noaa.gov/products/optimum-interpolation-sst

Smith, K. E., Burrows, M. T., Hobday, A. J., Sen Gupta, A., Moore, P. J., Thomsen, M., Wernberg, T., & Smale, D. A. (2021). Socioeconomic impacts of marine heatwaves: Global issues and opportunities. *Science*, *374*(6566), eabj3593. https://doi.org/10.1126/science.abj3593

W. Schlegel, R., & J. Smit, A. (2018). heatwaveR: A central algorithm for the detection of heatwaves and cold-spells. *Journal of Open Source Software*, *3*(27), 821. https://doi.org/10.21105/joss.00821